Microchimica Acta (2020) 187: 45
https://doi.org/10.1007/s00604-019-3829-3

ORIGINAL PAPER

A nanocomposite prepared from hemin and reduced graphene oxide foam for voltammetric sensing of hydrogen peroxide

Qinglian Li[1] · Yao Zhang[1] · Pengwei Li[1] · Huaiguo Xue[2] · Nengqin Jia[1]

Received: 7 May 2019 / Accepted: 14 September 2019 / Published online: 13 December 2019

Abstract

A foam consisting of reduced graphene oxide was synthesized by a one-pot hydrothermal method. The foam was used to prepare a nanocomposite with hemin which is formed via π-interactions. The nanocomposite was incorporated via a Nafion film and then placed on a glassy carbon electrode (GCE). The modified GCE displays outstanding catalytic activity towards H_2O_2. It is assumed that this is due to (a) the redox-active center [Fe(III/II)] of hemin, and (b) the crosslinked macroporous structure of the foam. Both improve the electron transfer rate and electrochemical signals. Under the optimum experimental conditions and a working voltage of typically −0.41 mV (vs. SCE), the sensor has a 2.8 nM H_2O_2 detection limit, and the analytically useful range extends from 5 nM to 5 mM with a sensitivity of 50.5 μA μM^{-1} cm^{-2}. The modified GCE has high sensitivity and fast response. It was utilized to quantify H_2O_2 in spiked environmental water samples.

Keywords One-pot hydrothermal method · Nanocomposite · H_2O_2 · Electrochemical sensor · π-Interactions

Introduction

Hydrogen peroxide (H_2O_2) is an indispensable intermediate or end product in chemical reactions and in industry. At the same time, it is also widely used in many fields, such as foodstuffs, medication, industrial engineering, environmental governance [1–3]. If the concentration of H_2O_2 exceeds a certain level, it can pose a threat to the life activities of animals and plants or human beings [4]. At present, a lot of methods have been developed, involving electrochemical [5], titrimetry [6], colorimetric detection [7], fluorometry [8]. For example, Jiang et al. [9] reported Ag nanoparticles modified conducting hydrogel was synthesized to detect H_2O_2 from living cells by means of electrochemiluminescence. Dou groups [10] developed a novel sensor, modified by a trimetallic hybrid nanoflower supported MoS_2 nanosheet, to monitor H_2O_2 from cancer cells. Shimeles and co-workers [11] described a sensor constructed by stainless steel electrode to detect the concentrated H_2O_2 via electrochemical measure. Zhu et al. [12] utilized chemiluminescence method to detect H_2O_2, using N-(amino butyl)-N-(ethanophenol) (ABEI) moderated gold nanoparticles AuNPs in ABEI/AuNPs/CoS_2 NWs.

Researchers are extensively attracted by electroanalysis owing to its intrinsic advantage, including high sensitivity, low-cost, relatively stable and real-time detection [13]. Especially enzymatic sensor, it has high sensitivity and accuracy. In spite of this, the enzymatic sensor has the inevitable disadvantage of enzyme instability and great environmental interference, which impose restrictions upon detection of H_2O_2 in actual application [14].

Among diversified materials, graphene and its composites have attracted great attention. In virtue of its marked performances, including large surface area, remarkable conductivity and high electron transfer rate [15], makes it possible in many

Electronic supplementary material The online version of this article (https://doi.org/10.1007/s00604-019-3829-3) contains supplementary material, which is available to authorized users.

✉ Huaiguo Xue
chhgxue@yzu.edu.cn

✉ Nengqin Jia
nqjia@shnu.edu.cn

[1] The Education Ministry Key Laboratory of Resource Chemistry, Shanghai Key Laboratory of Rare Earth Functional Materials, College of Chemistry and Materials Science, Shanghai Normal University, Shanghai 200234, People's Republic of China

[2] College of Chemistry & Chemical Engineering, Yangzhou University, Yangzhou 225002, China

fields. The three-dimensional reduced graphene oxide foam (3D rGO foam) contains abundant groups containing epoxy and hydroxyl groups [16], which are not only to covalently combine with the supported material, but also improve the solubility of the carrier substances. It is worth mentioning that 3D rGO foam has a cross-linked macroporous structure, which can enhance the electron transfer rate [17]. Simultaneously, it offers a possibility to support the more electroactive materials to improve sensitivity. For example, Ding et al. [18] designed a nanocomposite material, which was composed of amorphous carbon (AC) coated with Fe_3O_4 nanospheres and further sealed on the 3D rGO foam, to raise the electrical conductivity in lithium-ion batteries. Zhao groups [19] reported a hybrid aerogels, which was consisted of 3D rGO foam modified by Ti_3C_2Tx MXene, has good electromagnetic interference shielding performances. Xiao and coworkers [20] developed a 3D rGO-MoS_2/Pyramid Si heterojunction to enhance charge separation and transfer for the fabrication of optoelectronic devices.

Hemin, iron (III) protoporphyrin, has the center of redox activity, like some kinds of proteins, such as cytochrome c and peroxidases, can catalyze some substances. In addition, the electrocatalytic mechanism of hemin is similar to that of some enzymes, including peroxidase or nitrite reductase. It offers a probability for the H_2O_2, NO/NO_2, peroxide and tryptophan. Because of the characteristics of hemin, it possessed meaningful applications in the field of material analysis.

Herein, we devised an electrochemical sensor based on 3D rGO foam-hemin nanocomposites to detect different concentrations of H_2O_2. 3D rGO foam was prepared by the aid of hydrothermal process, which has a large specific surface area and can modify more electroactive substances to prevent the polymerization of materials [4]. Hemin, an electroactive substance, was immobilized on the 3D rGO foam by covalent bonding. Compared with enzyme-based sensor, the sensor has lower detection limit and prominent selectivity ability. It is worth mentioning that the performance of the sensor is relatively stable and less affected by environmental factors. This method can be used to synthesize different composite materials, such as hemoglobin (Hb), V_2O_5 nanozymes, Cu_2O [4, 21, 22], by loading corresponding electroactive substances.

Experimental section

Materials

Hemin (≥95%) was afforded from Shanghai Macklin Biochemical Co., Ltd. (http://www.macklin.cn/) Graphene Oxide (GO) was acquired from Shenzhen Tuling Evolution Technology Co., Ltd. (China). Nafion ® 117 solution and Uric acid (≥99%) were acquired from Sigma–Aldrich (https://www.sigmaaldrich.com/china-mainland.html). H_2O_2 (AR, 30%) and $NaH_2PO_4{\cdot}2H_2O$ were supplied from Sinopharm Chemical Reagent Co., Ltd. (http://en.reagent.com.cn/). $Na_2HPO_4{\cdot}2H_2O$ was provided by Shanghai qingjie chemical technology Co. Ltd. L-cysteine (99%) was accommodated from Aladdin (https://www.aladdin-e.com/). Ascorbic acid was gained from Shanghai chemical reagent factory (https://www.sinoreagent.com/). Overall aqueous solution were prepared by DI water.

Instrumentation

Cyclic Voltammetry (CV) curves was carried out on a CHI 660b electrochemical workstation (CH Instruments, Shanghai). The morphologies of 3D rGO foam and 3D rGO foam-hemin were investigated on a Hitachi S-4800 scanning electron microscopy (SEM). UV–vis spectrum was completed by a Thermo Multiskan spectrum spectrophotometer. Electrochemical impedance spectroscopy (EIS) curves was implement on a CHI 660b electrochemical workstation. Electrochemical measurements were accomplished via three electrode system, which consisted of active materials served as working electrode, a platinum functioned as auxiliary electrode and a SCE (saturated calomel electrode) as reference electrode.

Preparation of 3D rGO foam-hemin composites

In a typical procedure, the 3D rGO foam was prepared via a one-step hydrothermal method [23]. Firstly, 0.09 g of GO was put in 40 mL of ultrapure water and stirred at room temperature until the mixture was a uniform yellow solution. Afterwards, the GO aqueous dispersion was diverted to a 50 mL autoclave, which was retained at 160 °C up to 10 h. The columned self-assembled graphene hydrogel (SGH) was taken out from autoclave, when cooling to indoor temperature. The 3D rGO foam was generated through drying SGHs in a freeze dryer for 48 h to remove excess moisture. 1.0 mg of 3D rGO foam was resolved into 1 mL of ethanol solution containing 5 wt% Nafion via sonicating for 30 min to form well-proportioned solution. Then, 2.5 mg of hemin was dispersed to the mixture solution. To ensure a homogeneous solution, an ultrasound of the solution was performed for 30 min. After mixing evenly, the 3D rGO foam-hemin composites were eventually obtained, then stored in a 4 °C refrigerator for later use. Before each use, the mixed solution was ultrasonic for 10 min in the ultrasonic instrument to make it re-dispersed uniformly.

Fabrication 3D rGO foam-hemin sensor

Primarily, GCE was physically polished with 0.3 μm, 0.05 μm alumina powder separately, which was thoroughly rinsed with ethanol for several times, sonicated in ultrapure water for 2 min to remove of residues, followed by de-aerating with nitrogen gas. Before using the composite material, the composite material was ultrasonic in ultrasonic cleaner for 10 min to make the solution more evenly mixed. Afterwards, 4 μL of aforementioned 3D rGO foam-hemin nanocomposites were dripped to on the surface of the as-polished GCE. Finally, these modified electrodes were dried at 40 °C for 15 min in an oven. When being prepared completely, the modified electrodes were stocked in a refrigerator for later use.

Results and discussion

Characterizations of the 3D rGO foam and 3D rGO foam-hemin composites

Described by the Scheme 1 is constructed of this electrochemical sensor based on 3D rGO foam-hemin nanocomposites to detect the H_2O_2. The successful synthesis of 3D rGO foam is mainly ascribed to the recovery of π-conjugated system from GO sheets. In the reaction process, water can be retained in the reduced GO sheets, owing to the presence of incompletely reacted hydrophilic oxygen functional groups [24]. Therefore, the 3D rGO foam was prepared successfully attribute to this factor and π- stacking on reduced graphene oxide sheets. Hemin (iron porphyrin) is the active center of peroxidase, which is a carrier for electron transfer reaction. It has redox properties based on changes in the valence state of iron. Compared with enzyme, hemin is not easily influenced through environmental element containing temperature and pH, which makes the performance of sensor more stable and avoid external interference. Thus, hemin instead of enzyme was selected to fabricate sensor. To deserve to be mentioned, 3D rGO foam combine with hemin firmly via the π–interactions [25]. Nafion is a perfluorinated sulfonate polyelectrolyte. The volatile film can fix some electroactive substances firmly through ion exchange to avoid the modified material leakage. Therefore, Nafion is used as bonding stabilizer to fix electroactive substances on the surface of the GCE to avoid the modified material leaks from the electrode surface.

The morphology of 3D rGO foam and 3D rGO foam-hemin composites are revealed via SEM. Figure 1a exhibits that freeze-dried samples possess plenty of porous structures with pore sizes of the skeleton ranging from several hundred nanometers to several micrometers. Figure 1b with high magnification displays that a well-defined 3D rGO foam are composed of abundant thin layers of GO stacked nanosheets. Due to the convergence of graphene sheets, the mechanical cross-linking sites of 3D rGO foam were formed. Accordingly, the fabrication of macroporous graphene sheets has considerable intrinsic flexibility. As shown in Fig. 1c, a large amount of hemin is randomly dispersed in the 3D rGO foam, and significantly, the 3D rGO foam retains its inherent structure even after hemin immobilization. This phenomenon proves that the 3D rGO foam not only has strong mechanical strength, but also possesses a large specific surface area to support more hemin. Furthermore, the rod-shaped structure of hemin adsorbed on the 3D rGO foam is monodispersed without obvious aggregation, as shown in Fig. 1d. At the same time, from the SEM, we can intuitively see the successful preparation of composite materials, which can be further verified by UV-vis absorption spectroscopic results(Fig.S1).

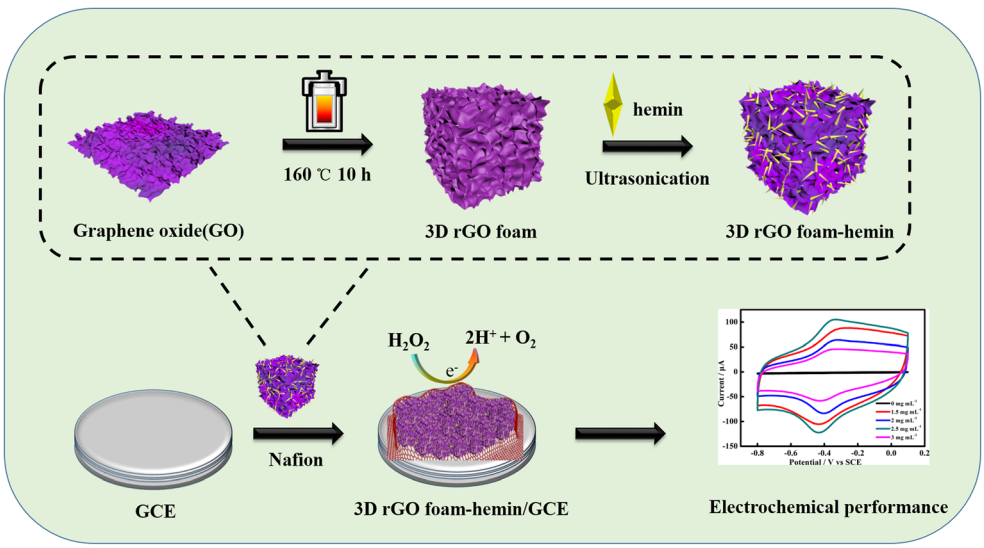

Scheme 1 Schematic presentation of the electrochemical hydrogen peroxide sensor based on a nanocomposite prepared from hemin and reduced graphene oxide foam

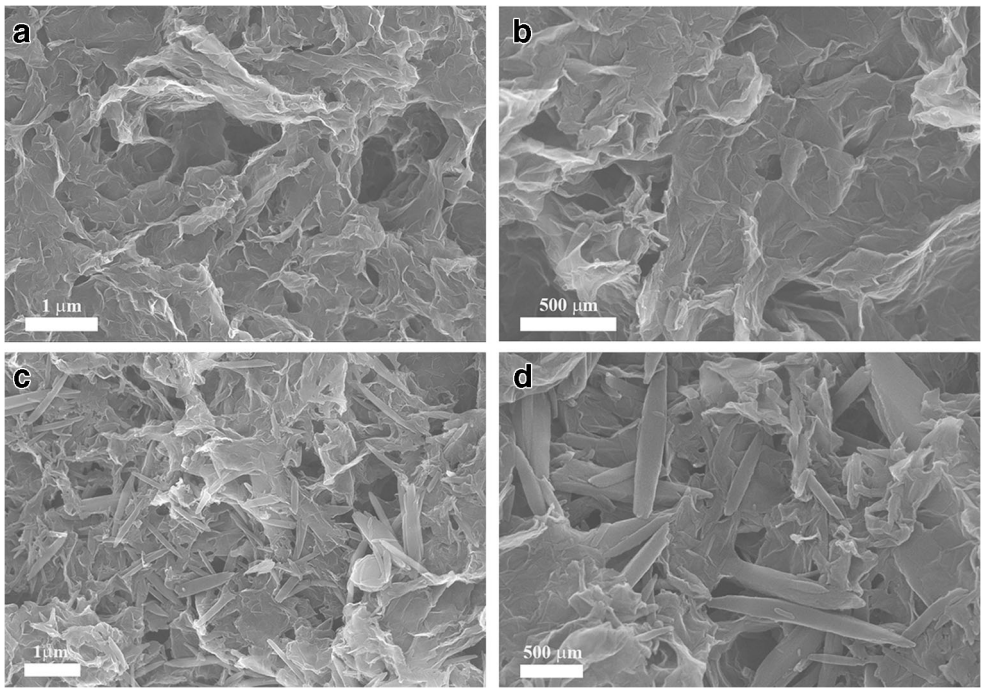

Fig. 1 SEM images of 3D rGO foam (**a** and **b**) and 3D rGO foam-hemin (**c** and **d**) at different magnifications

Electrochemical characterizations

To evaluate the catalytic performance of hemin and its composites, the electrochemical means of Cyclic Voltammetry (CV) was employed. Figure 2a shows CV curves of different modified electrodes in N_2-saturated PBS (0.1 M, pH 7.0) at scan rate of 100 mV s^{-1}. As is shown, the bare electrode and the 3D rGO foam modified electrode present relative flat curves of double-layer charging, while the hemin and its composites electrode conduct redox peaks under the same

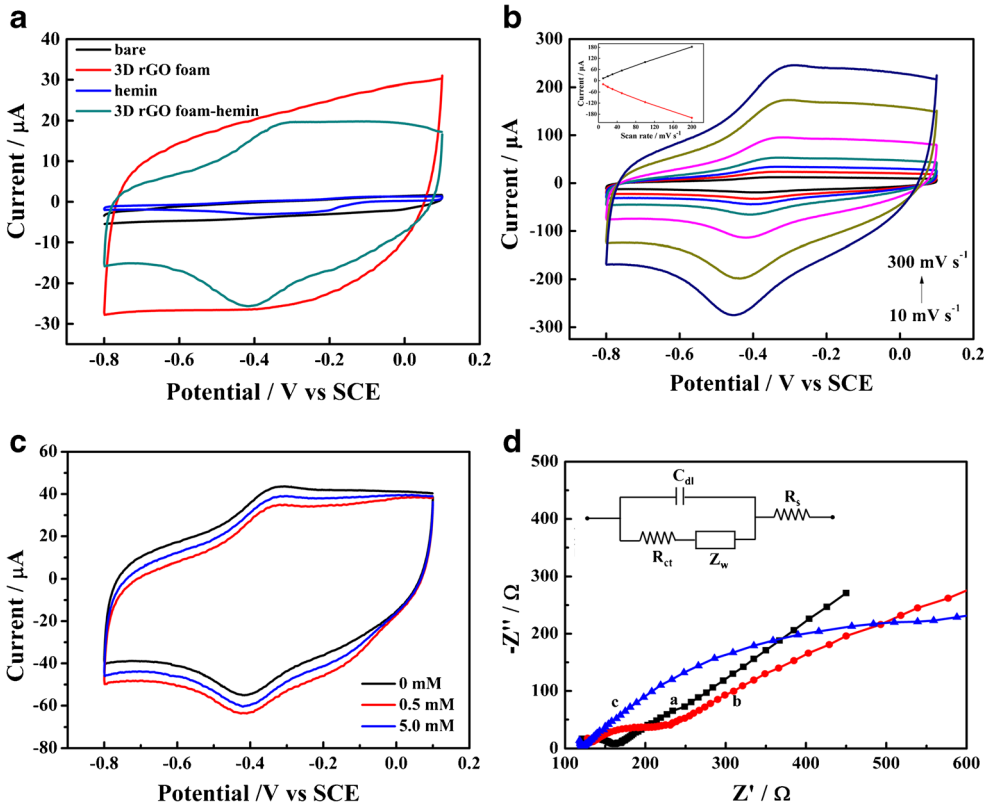

Fig. 2 **a** CV curves of the bare, 3D rGO foam, hemin, 3D rGO foam-heminat the scan rate of 100 mV s^{-1}. **b** CV curves of the 3D rGO foam-hemin electrode recorded at different scan rates (from inner to outer: 10, 20, 30, 50, 100, 200, 300 mV s^{-1}) in N_2-saturated PBS (0.1 M, pH 7.0). Inset: plots of peak currents versus scan rate. **c** CV curves of the 3D rGO foam-hemin electrode recorded at different concentrations of H_2O_2 at the scan rate of 100 mV s^{-1} in the scan range from −0.8 V to 0.1 V. **d** Electrochemical impedance spectroscopy of (a) bare GCE, (b) 3D rGO foam/GCE, (c) 3D rGO foam-hemin/GCE in 5.0 mM $K_3Fe(CN)_6/K_4Fe(CN)_6$ (1:1). Inset is corresponding equivalent circuit

condition. The redox peak of the 3D rGO foam-hemin/GCE curve is clearly visible, with the oxidation peak approximately −0.309 V and the reduction peak approximately-0.409 V. As a result, the formal potential $E^{0'}$ is calculated to be −0.359 V by the formula of $E^{0'} = (E_{pa} + E_{pc})/2$, which is in keeping with the previously reported hemin redox pair. The issue strongly assumes that the 3D rGO foam as a substrate can accomplish the goal of direct electron transfer (DET) between the hemin and GCE, which ascribes to redox reaction of hemin active center: $Fe(III) + e^{-} \rightarrow Fe(II)$. The peak current rate (I_{pc}/I_{pa}) of 3D rGO foam-hemin/GCE is 1.3, while hemin/GCE drops down to 1.02. The peak potential difference (ΔE_p) rises from 38 mV for hemin/GCE to 100 mV for 3D rGO foam-hemin/GCE. In brief, compared with hemin, the 3D rGO foam-hemin/GCE performs an apparent increase of peak current. Cathodic and anodic peak currents of 3D rGO foam-hemin are eight times higher than that of 3D rGO foam. This phenomenon is primarily due to the inherent properties of the 3D rGO foam, which has a continuous porous network that accelerates the charge transfer between hemin and GCE. On the basis of Laviron's equation: [26].

$$logk_s = \alpha log(1-\alpha) + (1-\alpha)log\alpha - log\left(\frac{RT}{nFv}\right) - \alpha(1-\alpha)\frac{nF\Delta E_p}{2.303RT} \quad (1)$$

in the system of 3D rGO foam-hemin/GCE, we assume the charge transfer coefficient $\alpha = 0.5$, charge transfer number $n = 1$ and the peak potential difference, $\Delta E_p = 100$ mV, k_s is estimated to be 0.736 s^{-1}, which is twice as much as the value of the individual hemin. This affirms that the foam has a large specific surface not only to immobilize more hemin, but also to prevent hemin aggregation and facilitate electron transfer. The surface (Γ) number of electroactive hemin immobilized on the surface of 3D rGO foam is figured up basing on the following expressions [26]:

$$I_p = 0.4463\left(\frac{F^3}{RT}\right)^{\frac{1}{2}} n^{\frac{3}{2}} v^{\frac{1}{2}} D_0^{\frac{1}{2}} AC_0 \quad (2)$$

Table 1 Comparison of the proposed sensor with other reported electrode materials for determination of H_2O_2

Electrode materials	Linear range	Detection (nM)	References
ABEI–Ag@PAni–PA	0.01–40 μM	3.3 nM	[9]
Ag/graphene oxide	100–2000 μM	1.9 μM	[28]
FePt-Au HNPs	20–700 μM	12.33 μM	[29]
PtPb/G	2 nM-2.5 mM	2 nM	[30]
3D rGO foam-hemin	5 nM-5 mM	2.83 nM	This work

Here, *n* stands for the number of electron transfers (n = 1), F is on behalf of Faraday constant (96,485 C mol^{-1}) and v represent the scan rate. The concentration of electroactive hemin at 3D rGO foam/GCE was evaluated to be 0.316 mol cm^{-2}, which is bigger than that of hemin/GCE (0.023 mol cm^{-2}). It is mainly attributed to plentiful pore structure of 3D rGO foam, more hemin can be decorated. Therefore, 3D rGO foam composites have favorable capabilities for the advanced accuracy in sensor applications and improve the sensitivity of the sensor.

Figure 2b manifests the CV of 3D rGO foam-hemin/GCE at different scan rates. The inset presents that current have linear relation with the scan rate increase. These phenomena expose that there is a direct electron transfer (DET) between the hemin and GCE, and the DET depends on the surface control process. The direct electrochemistry of 3D rGO foam-hemin suggests that 3D rGO foam can provide a suitable microenvironment for hemin DET. The peak potential difference has nothing to do with the scan rate, which indirectly point out that electrons can not only be transferred rapidly between hemin and GCE after doping 3D rGO foam, but also hemin can be firmly stabilized on 3D rGO foam. The fascinating electron transfer behavior vitalizes us to detect the sensor properties of the as-synthesized 3D rGO foam-hemin composites.

The electrochemical catalytic behavior of the 3D rGO foam-hemin/GCE sensor in H_2O_2 redox reaction is studied by CV method. As depicted in Fig. 2c, when there is no

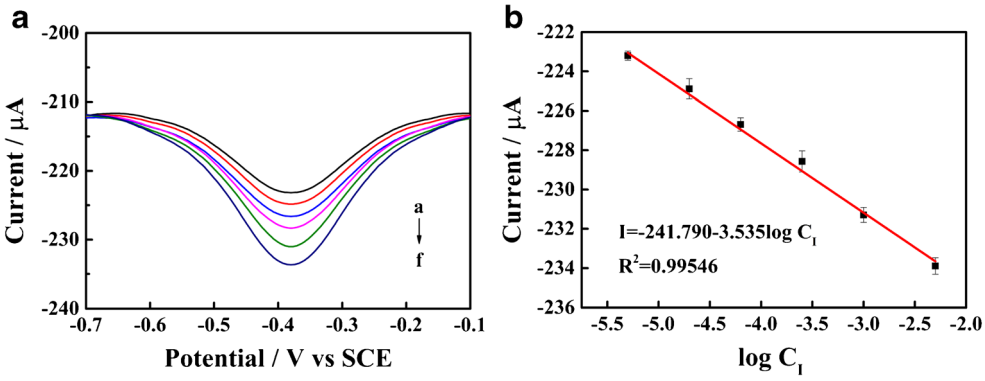

Fig.3 **a** Typical current-concentration response curves of the sensor measured by differential pulse voltammetry upon successive additions of H_2O_2. **b** The calibration plot for H_2O_2 in the linear range (5 nM-5 mM). Scan rate of 100 mVs^{-1} and the scan range from −0.7 V to −0.1 V

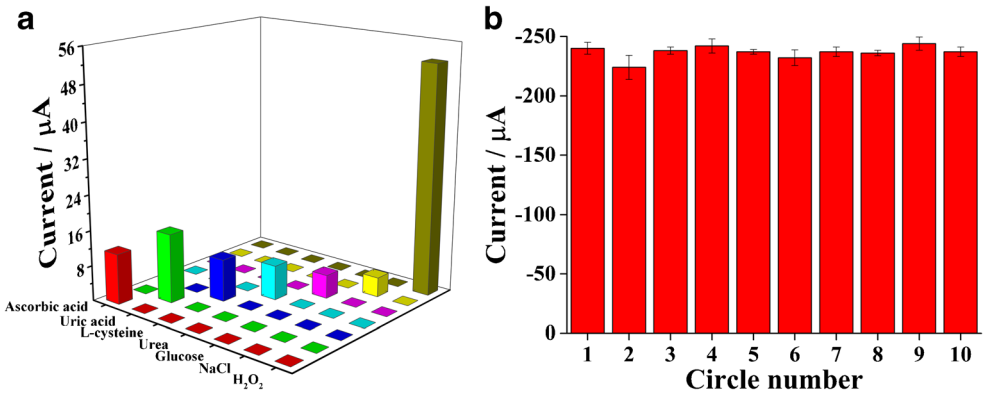

Fig.4 **a** Amperometric responses of 3D rGO foam-hemin for the sequential addition of 100 nM Ascorbic acid, 100 nM Uric acid, 100 nM L-Cysteine, 100 nM Urea, 100 nM Glucose, 100 nM NaCl and 100 nM H_2O_2. **b** Cathodic current of 3D rGO foam-hemin electrode recorded at different circles ($n = 5$)

H_2O_2 in PBS, the modified electrode exhibits clearly defined redox peak at −0.409 V and − 0.309 V, separately. With the concentration of H_2O_2 increasing, the CV curve of the 3D rGO foam-hemin/GCE displays an increased anodic and cathodic peak current, which indicates that H_2O_2 on the 3D rGO foam-hemin/GCE is obviously oxidized and reduced. This is mostly because that the H_2O_2 was catalyzed by electroactive substance hemin to produce an enhanced current signal. Accordingly, the current intensity enhances with the concentration of H_2O_2. The hemin catalytic mechanism of H_2O_2 redox reaction is arranged as follows [27]:

$$hemin(FeIII) + H_2O_2 \rightarrow hemin(FeII) + H_2O \quad (3)$$

$$hemin(FeIII) + e^- \rightarrow hemin(FeII) \quad (4)$$

$$\frac{1}{2}H_2O_2 + H^+ + e^- \rightarrow H_2O \quad (5)$$

$$H_2O \rightarrow \frac{1}{2}H_2O_2 + H^+ + e^- \quad (6)$$

$$hemin(FeII) \rightarrow hemin(FeIII) + e^- \quad (7)$$

Figure 2d indicates the EIS curves via utilizing $[Fe(CN)_6]^{3-/4-}$ as signal probe. The Nyquist plots of the modified electrodes are composed of the high frequency semicircle corresponding to the electron transfer restriction process and the low frequency linear part corresponding to the diffusion process. The electron transfer resistance (Rct) of 3D rGO foam-hemin composites modified electrode can be acquired from the semicircle diameter. As revealed in Fig. 2d, the electron transfer resistance of the bare electrode displays a fairly low electron-transfer resistance 25 Ω (curve a). As the 3D rGO foam modified, the resistance increases around 60 Ω (curve b), just that the negative charge of the oxygenated functional groups may exist an electrostatic repulsion between 3D rGO foam and redox probe, causing the resistance increases. When embedded the hemin, the electron-transfer resistance of the 3D rGO foam-hemin/GCE exhibits a higher value about 210 Ω (curve c). The consequence may be ascribed to hemin is a macromolecule protein with poor electrical conductivity that hinders electron transfer. The consequence testify the triumphant arrangement of 3D rGO foam-hemin composites.

Table 2 The recoveries of H_2O_2 in the serum determined by the proposed 3D rGO foam-hemin-based electrochemical sensor

Sample	C_{added} nM	C_{detect} nM	Recovery (%)	R.S.D (%)
1	10	9.26	92.6	4.13
2	100	102.7	102.7	3.68
3	500	484.6	96.9	2.55
4	600	607.4	101.2	5.41

Optimization of the assay

In order to examine the domino offect of the concentration of hemin on the characteristic of the sensor, we selected the concentrations of hemin and 3D rGO foam in various proportions as the control experiment. Specifically, the concentration of 3D rGO foam is constantly (1 mg mL^{-1}) immobilized with different concentrations of hemin. Hemin contains Fe(III) porphyrin. Hence, the DET between hemin and GCE is affected by pH. In order to accomplish this, different pH were surveyed by CV. Relevant data and Figures on optimizations are placed in the Electronic Supporting Material (Fig. 2S). In a word, the experimental results shows that the optimum dosage: (a) 2.5 mg of hemin and 1.0 mg of 3D rGO foam; (b) the best pH value of 7.

Quantitative experiments

Figure 3 reveals a typical response for the 3D rGO foam-hemin/GCE upon successive additions of H_2O_2 under stirring in N_2-saturated PBS. A given mass of H_2O_2 solution was added to the agitated PBS, the cathodic current obviously increased and the reaction was rapid. The calibration diagram of the 3D rGO foam-hemin/GCE sensor consistent with the amperometric response, as is illustrated in Fig. 3, displays a large linear range of 5 nM-5 mM ($R^2 = 0.99546$) and the detection limit is 2.83 nM with the signal to noise ratio(S/N) of 3. Furthermore, with the comparisons of different electrode

materials for H_2O_2 (Table 1), the proposed sensor displayed several superior analytical performances including relatively low detection limit and wide linear range.

From the aforementioned consequences, we can draw a conclusion that 3D rGO foam-hemin/GCE sensor illuminates superior performances, owing to the special properties of 3D rGO foam, including a large active surface area can be embedded more electroactive material hemin, high electrical conductivity raises the sensitivity and mechanically strong provides a stable environment. It offers a potential for detecting low concentration relative to other electrode materials. Besides, hemin is different from enzyme, its properties are more stable. It is not easy to inactivate, and it can catalyze H_2O_2 effectively. These inherent excellent properties provide a possible factor to build a sensitive electrochemical sensor.

Selectivity, stability and real-sample analysis

We put the sensor into the interfering substance to check on the practicability of the sensor. As the Fig. 4a displayed, the amperometric response of 3D rGO foam-hemin modified GCE toward H_2O_2 and other interfering substance at a scanning potential between −0.8 V and 0.1 V. After adding the 100 nM of ascorbic acid, 100 nM of uric acid and 100 nM of L-cysteine, 100 nM urea, 100 nM glucose, 100 nM NaCl compared with the blank experiment. The reduction current increases slightly or even decreases. Notably, the addition of 50 nM of H_2O_2 results in a fairly evident increase in reduction current compared with other substances. These results can prove that the modified sensor has a pretty selectivity toward H_2O_2. Subsequently, stability and real-sample analysis of the sensor were valued in the following experiment. The relative standard deviation (RSD) of the sensor for repeated determination of H_2O_2 (50 nM) was 5.2% ($n = 5$). This value is similar to that of partially commercialized H_2O_2 sensor, indicating that the sensor has good reproducibility.

To prove the practical applicability of the sensor, serum was used as the real sample, which contains plenty of potentially interfering ions. It can be seen from the Table 2, when different concentration of H_2O_2 (10–600 nM) was respectively added into the serum samples, the recoveries are ranged from 92.6% to 102.7%. These phenomena indicated the sensor can be applied for the determination of H_2O_2 in practical use.

Conclusion

We describe a sensitive sensor rested on nanostructured 3D rGO foam-hemin hybrid for H_2O_2. 3D rGO foam was synthesized by hydrothermal method owing to hydrophilic oxygenated groups, can encapsulate water and π-stacking of graphene sheets. The assembly of hemin on 3D rGO foam is mainly driven by the π-stacking on reduced graphene oxide sheets. The covalent functionalization of 3D rGO foam improves the stability of hemin, at the same time, it can sustain its good conductivity. The as-synthesized 3D rGO foam proves to be a satisfying matrix between protein and GCE direct electron transfer. 3D rGO foam-hemin modified electrode has a well-defined direct electrochemical behavior. With an interconnected network of 3D rGO foam makes the active sites of hemin exposure and accelerate the electron transfer, the sensor has a marked performance. The 3D rGO foam-hemin-based sensor shows salient catalytic activity toward H_2O_2 reduction. The phenomenon suggests that 3D rGO foam acts as a good electrical conductor. 3D rGO foam functions as an environmentally friendly matrix, which offers a beneficial microenvironment for immobilizing protein to maintain its bioactivity and fulfil fast DET as well as becoming a potential material for electrochemical sensors. In addition, 3D rGO foam with excellent properties can be put into many domain, including bioengineering and energy storage, such as drug transport, biomimetic nanomaterials, supercapacitors. We can design 3D rGO foam as the substrate material to immobilize different electroactive materials. It provides a potential possibility for practical production.

Acknowledgements We gratefully acknowledge the financial support from the Shanghai Science and Technology Committee (Grant No. 17070503000, 18dz2308700); Program for Changjiang Scholars and Innovative Research Team in University (IRT_16R49); International Joint Laboratory on Resource Chemistry (IJLRC) and Shanghai Engineering Research Center of Green Energy.

Compliance with ethical standards

Conflict of interest The author(s) declare that they have no competing interests.

References

1. Sun LF, Ding YY, Jiang YL, Liu QY (2017) Montmorillonite-loaded ceria nanocomposites with superior peroxidase-like activity for rapid colorimetric detection of H_2O_2. Sensors Actuators B Chem 239:848–856. https://doi.org/10.1016/j.snb.2016.08.094
2. Muralikrishna S, Cheunkar S, Lertanantawong B, Ramakrishnappa T, Nagaraju DH, Surareungchai W, Balakrishna RG, Reddy KR (2016) Graphene oxide-Cu(II) composite electrode for non-enzymatic determination of hydrogen peroxide. J Electroanal Chem 776:59–65. https://doi.org/10.1016/j.jelechem.2016.06.034
3. Xu FG, Deng M, Li GY, Chen SH, Wang L (2013) Electrochemical behavior of cuprous oxide–reduced graphene oxide nanocomposites and their application in nonenzymatic hydrogen peroxide sensing. Electrochim Acta 88:59–65. https://doi.org/10.1016/j.electacta.2012.10.070
4. Sun JH, Li CY, Qi YF, Guo SL, Liang X (2016) Optimizing colorimetric assay based on V_2O_5 nanozymes for sensitive detection of H_2O_2 and glucose. Sensors 16:584. https://doi.org/10.3390/s16040584

5. Wang CH, Yang C, Song YY, Gao W, Xia XH (2005) Adsorption and direct electron transfer from hemoglobin into a three-dimensionally ordered macroporous gold film. Adv Funct Mater 15:1267–1275. https://doi.org/10.1002/adfm.200500048
6. Klassen NV, Marchlngton D, McGowan HCE (1994) H_2O_2 determination by the I_3^- method and by $KMnO_4$ titration. Anal Chem 66:2921–2925. https://doi.org/10.1021/ac00090a020
7. Liu QY, Yang YT, Lv XT, Ding YN, Zhang YZ, Jing JJ, Xu CX (2017) One-step synthesis of uniform nanoparticles of porphyrin functionalized ceria with promising peroxidase mimetics for H_2O_2 and glucose colorimetric detection. Sensors Actuators B Chem 240: 726–734. https://doi.org/10.1016/j.snb.2016.09.049
8. Zhang WC, Niu XH, Li X, He YF, Song HW, Peng YX, Pan JM (2018) A smartphone-integrated ready-to-use paper-based sensor with mesoporous carbon-dispersed Pd nanoparticles as a highly active peroxidase mimic for H_2O_2 detection. Sensors Actuators B Chem 265:412–420. https://doi.org/10.1016/j.snb.2018.03.082
9. Jiang X, Wang HJ, Yuan R, Chai YQ (2018) Functional three-dimensional porous conductive polymer hydrogels for sensitive electrochemiluminescence in situ detection of H_2O_2 released from live cells. Anal Chem 90:8462–8469. https://doi.org/10.1021/acs.analchem.8b01168
10. Dou BT, Yang JM, Yuan R, Xiang Y (2018) Trimetallic hybrid nanoflower-decorated MoS_2 nanosheet sensor for direct in situ monitoring of H_2O_2 secreted from live cancer cells. Anal Chem 90:5945–5950. https://doi.org/10.1021/acs.analchem.8b00894
11. Kitte SA, Zafar MN, Zholudov YT, Ma X, Nsabimana A, Zhang W, Xu GB (2018) Determination of concentrated hydrogen peroxide free from oxygen interference at stainless steel electrode. Anal Chem 90:8680–8685. https://doi.org/10.1021/acs.analchem.8b02038
12. Zhu QJ, Huang JS, Yan MX, Ye J, Wang DW, Lu QQ, Yang XR (2018) N-(Aminobutyl)-N-(ethylisoluminol)-functionalized gold nanoparticles on cobalt disulfide nanowire hybrids for the non-enzymatic chemiluminescence detection of H_2O_2. Nanoscale 10: 14847–14851. https://doi.org/10.1039/c8nr03990a
13. Feng QM, Shen YZ, Li MX, Zhang ZL, Zhao W, Xu JJ, Chen HY (2016) Dual-wavelength electrochemiluminescence ratiometry based on resonance energy transfer between Au nanoparticles functionalized g-C_3N_4 nanosheet and $Ru(bpy)_3^{2+}$ for microRNA detection. Anal Chem 88:937–944. https://doi.org/10.1021/acs.analchem.5b03670
14. Liu YD, Shang TY, Liu YL, Liu XH, Xue ZH, Liu XH (2018) Highly sensitive platinum nanoparticles-embedded porous graphene sensor for monitoring ROS from living cells upon oxidative stress. Sensors Actuators B Chem 263:543–549. https://doi.org/10.1016/j.snb.2018.02.135
15. Kang Z, Li Y, Cao SY, Zhang ZH, Guo HJ, Wu PW, Zhou LX, Zhang SC, Zhang XM, Zhang Y (2018) 3D graphene foam/ZnO nanorods array mixed-dimensional heterostructure for photoelectrochemical biosensing. Inorg Chem Front 5:364–369. https://doi.org/10.1039/c7qi00669a
16. Hou YB, Sheng K, Lu Y, Ma C, Liu W, Men XJ, Xu L, Yin SY, Dong B, Bai X, Song HW (2018) Three-dimensional graphene oxide foams loaded with AuPd alloy: a sensitive electrochemical sensor for dopamine. Microchim Acta 185:397. https://doi.org/10.1007/s00604-018-2925-0
17. Li N, Jiang HL, Wang XL, Wang X, Xu GJ, Zhang BB, Wang LJ, Zhao RS, Lin JM (2018) Recent advances in graphene-based magnetic composites for magnetic solid-phase extraction. Trends Anal Chem 102:60–74. https://doi.org/10.1016/j.trac.2018.01.009
18. Ding RR, Zhang J, Qi J, Li ZH, Wang CY, Chen MM (2018) N-doped dual carbon-confined 3D architecture rGO/Fe_3O_4/AC nanocomposite for high-performance lithium-ion batteries. ACS Appl Mater Interfaces 10:13470–13478. https://doi.org/10.1021/acsami.8b00353
19. Zhao S, Zhang HB, Luo JQ, Wang QW, Xu B, Hong S, Yu ZZ (2018) Highly electrically conductive three-dimensional $Ti_3C_2T_x$ MXene/reduced graphene oxide hybrid aerogels with excellent electromagnetic interference shielding performances. ACS Nano 12:11193–11202. https://doi.org/10.1021/acsnano.8b05739
20. Xiao P, Mao J, Ding K, Luo WJ, Hu WD, Zhang XJ, Zhang XH, Jie JS (2018) Solution-processed 3D rGO–MoS_2/pyramid Si heterojunction for ultrahigh detectivity and ultrabroadband photodetection. Adv Mater 30:1801729. https://doi.org/10.1002/adma.201801729
21. Lu WD, Sun YJ, Dai HC, Ni PJ, Jiang S, Wang Y, Li Z, Li Z (2016) Direct growth of pod-like Cu_2O nanowire arrays on copper foam: highly sensitive and efficient nonenzymatic glucose and H_2O_2 sensor. Sensors Actuators B Chem 231:860–866. https://doi.org/10.1016/j.snb.2016.03.058
22. Zhao Y, Hu CG, Hu Y, Cheng HH, Shi GQ, Qu LT (2012) A versatile, ultralight, nitrogen-doped graphene framework. Angew Chem Int Ed 51:11371–11375. https://doi.org/10.1002/anie.201206554
23. Xu YX, Sheng KX, Li C, Shi GQ (2010) Self-assembled graphene hydrogel via a one-step hydrothermal process. ACS Nano 4(7): 4324–4330. https://doi.org/10.1021/nn101187z
24. Jiang XY, Chai YQ, Wang HJ, Yuan R (2014) Electrochemiluminescence of luminol enhanced by the synergetic catalysis of hemin and silver nanoparticles for sensitive protein detection. Biosens Bioelectron 54:20–26. https://doi.org/10.1016/j.bios.2013.10.006
25. Xu YF, Liu ZB, Zhang XL, Wang Y, Tian JG, Huang Y, Ma YF, Zhang XY, Chen YS (2009) A graphene hybrid material covalently functionalized with porphyrin: synthesis and optical limiting property. Adv Mater 21:1275–1279. https://doi.org/10.1002/adma.200801617
26. Narayana PV, Reddy TM, Gopal P, Raghu P, Reddaiah K, Srinivasulu M (2014) Development of trypan blue polymer film based electrochemical sensor for the determination of dopamine and its simultaneous detection in presence of ascorbic acid and uric acid: a voltammetric method. Anal Bioanal Electrochem 6:485–500. https://doi.org/10.1016/j.aca.2013.06.016
27. Palanisamy S, Velusamya V, Chen SW, Yang TCK, Balu S, Banks CE (2019) Enhanced reversible redox activity of hemin on cellulose microfiber integrated reduced graphene oxide for H_2O_2 sensor applications. Carbohydr Polym 204:152–160. https://doi.org/10.1016/j.carbpol.2018.10.001
28. Lu W, Chang G, Luo Y, Liao F, Sun XJ (2011) Method for effective immobilization of Ag nanoparticles/graphene oxide composites on single-stranded DNA modified gold electrode for enzymeless H_2O_2 detection. Mater Sci 46:5260–5266. https://doi.org/10.1007/s10853-011-5464-1
29. Ding YN, Yang BC, Liu H, Liu ZX, Zhang X, Zheng XW, Liu QY (2018) FePt-au ternary metallic nanoparticles with the enhanced peroxidase-like activity for ultrafast colorimetric detection of H_2O_2. Sensors Actuators B Chem 259:775–783. https://doi.org/10.1016/j.snb.2017.12.115
30. Sun YJ, Luo MC, Meng XX, Xiang J, Wang L, Ren QS, Guo SJ (2017) Graphene/intermetallic PtPb nanoplates composites for boosting electrochemical detection of H_2O_2 released from cells. Anal Chem 89:3761–3767. https://doi.org/10.1021/acs.analchem.7b00248